

PEVLM: Parallel Encoding for Vision-Language Models

Letian Kang*, Shixian Luo, Yiqiang Li, Xiaoyang Yu, Shenxuan Zhou, and Yong Wu
Li Auto Inc.

Abstract

Vision-Language Models (VLMs) have demonstrated strong capabilities in multimodal understanding and generation tasks. However, their application to long video understanding remains hindered by the quadratic complexity of standard attention mechanisms. In this work, we introduce **PEVLM**, a fine-tuning-free parallel encoding method designed to enhance the prefilling efficiency of VLMs in long video scenarios. PEVLM partitions the input video into context blocks with a shared sink block, while preserving sequential position embeddings to align the attention weight distribution with that of Full-Attention. This design reduces attention complexity from $O((T \times N)^2)$ to $O(T \times N)$ where T is the number of frames and N the number of tokens per frame, without sacrificing accuracy. Extensive experiments across multiple state-of-the-art models and benchmarks demonstrate that PEVLM consistently outperforms existing parallel encoding approaches, achieving up to **7.47x** speedup in attention computation and reducing end-to-end latency by **40%**. Remarkably, PEVLM not only maintains high accuracy, but in some settings even surpasses Full-Attention performance. Under strict latency constraints, it achieves substantial gains, improving accuracy from **23.26%** to **61.03%**. These results underscore the effectiveness of PEVLM for low-latency, long-context video understanding, making it a promising solution for real-world applications.

Introduction

In recent years, Vision-Language Models (VLMs) have emerged as a central research focus at the intersection of computer vision and natural language processing, demonstrating impressive performance in multimodal understanding and generation tasks (Alayrac et al. 2022; Li et al. 2020; Radford et al. 2021; Zhu et al. 2023). As the capabilities of these models continue to strengthen, their application scenarios have also expanded, including robotics (Black, Lee et al. 2024; Cheang, Huang et al. 2024; Prasad, Singh et al. 2024), autonomous driving (Gao, Lin et al. 2024; Hu, Wu et al. 2023; Wang, Zhao et al. 2024), and healthcare (Liu, Zhang et al. 2024). Correspondingly, the length of the videos has also increased significantly.

However, applying VLMs to long-video data introduces a significant computational challenge: The quadratic complexity of transformer-based attention mechanisms causes

computation to scale rapidly with the input sequence length (Beltagy, Peters, and Cohan 2020; Vaswani et al. 2017), especially during the prefilling stage, where all input tokens must be processed before generating any output. This severely limits the scalability of VLMs in long-video understanding tasks. In practical scenarios where the entire video must be encoded before decoding begins—such as video captioning, retrieval, or reasoning—this inefficiency becomes a critical bottleneck. Therefore, optimizing the prefilling phase is essential to efficiently deploy VLMs on long video tasks.

A widely adopted technique in LLMs to speed up long context prefilling is the **parallel encoding** mechanism (Li et al. 2024b; Liu et al. 2024; Ma, Wang, and Tian 2025; Ratner et al. 2023; Yang, Chen, and Chen 2025; Yen, Gao, and Chen 2024; Lu et al. 2024). In these approaches, the input context is divided into blocks, and each block is encoded into Key-Value (KV) states independently. This means that tokens from different blocks do not attend to each other. Since the parallel encoding mechanism omits attention computation across blocks, it reduces the computational complexity from $O(L^2)$ to $O(L)$. The parallel encoding mechanism also mitigates the problem of "lost in the middle" (Liu et al. 2023), and in long-context scenarios, it can even achieve accuracy surpassing that of Full-Attention (Yang, Chen, and Chen 2025).

Several state-of-the-art architectural improvements have been proposed to enhance the parallel encoding mechanism. **Adaptive Parallel Encoding (APE)** improves prefilling efficiency by introducing shared prefixes, an attention temperature parameter, and a scaling factor to better align the distribution of attention weight in parallel encoding with that of sequential encoding. Although these adjustments improve accuracy, they are highly sensitive to length, quantity, and content, making them difficult to tune and deploy in practice (Yang, Chen, and Chen 2025). **Star Attention** extends ring attention by incorporating a parallel encoding strategy, which eliminates communication overhead during the prefilling stage and reduces overall computational complexity (Liu et al. 2024). Another notable distinction of Star Attention is the use of a larger sink size, which is equal to the block size. **Block-Attention & TurboRAG** share the same idea: build on parallel encoding, apply position re-encoding and fine-tune to improve accuracy (Guu et al. 2020; Lu et al. 2024). However, without fine-tune, the accuracy of both suf-

*Corresponding author: kangletian@lixiang.com

fers for the absence of a Sink Block. Nevertheless, the idea of preserving the sequential position embeddings for each block, rather than reusing a shared one, offers a valuable and insightful idea.

In addition, there are several widely discussed methods such as Native Sparse Attention (Yuan et al. 2025) from Deepseek and MoBA (Lu et al. 2025), which adopt similar algorithmic principles and achieve acceleration effects comparable to parallel encoding. However, both approaches involve modifications to the model architecture and thus require retraining from scratch. This poses a challenge for many inference platforms, which typically do not have control over users’ model preferences. The issue is particularly pronounced in domains such as autonomous driving, where a reliable models are often continuously trained and iterated over years. Consequently, we focus on finetune-free optimization methods to ensure compatibility and ease of deployment.

Given all of these, a key question naturally arises: **Can existing methods be directly applied to VLMs to accelerate inference and deployment pipelines?** In Table 1, we evaluate several models with existing parallel encoding methods on LongVideoBench (Zhang and Wang 2024), VideoMME (Fu et al. 2024), EgoSchema (Mangalam, Akshulakov, and Malik 2023) and MVBench (Li et al. 2024a) benchmarks. Although existing parallel encoding methods achieve some effectiveness in shorter videos, we observe varying degrees of accuracy degradation across different models on longer videos, particularly for Qwen2.5-VL. To investigate this issue, we analyze the attention weight distributions under parallel encoding and identify a misalignment between Full-Attention and parallel encoding. Existing methods developed for LLMs fail to effectively address this misalignment in VLMs. Building upon this observation. We conducted a series of studies and experiments and ultimately propose a novel attention mechanism for VLMs, termed **Parallel Encoding for Vision-Language Models (PEVLM)**. PEVLM is a fine-tuning-free method specifically designed to accelerate the prefilling stage in long-video processing with VLMs. Our contributions involve:

- We systematically analyze the distribution characteristics of attention weights under parallel encoding in VLMs. Our observations reveal a key reason for the misalignment between the attention weight distributions of parallel encoding and Full-Attention: the reuse of position embeddings across blocks leads to the loss of critical video information.
- We propose PEVLM to recover the accuracy of parallel encoding by applying three targeted alignment steps: (i) Segmenting contexts into blocks by video frames rather than tokens. (ii) Using the system prompts and the initial frames of the video as Sink Block for all blocks to avoid the duplication of abnormal distribution of initial tokens. (iii) Preserving the sequential position embeddings instead of resuing position embeddings across blocks. PEVLM achieves superior accuracy compared to other parallel-encoding-based methods on long video processing tasks, with up to a 9.73% improvement across different models.
- PEVLM reduces the computational complexity of the at-

tention mechanism from $O((T \times N)^2)$ to $O(T \times N)$, which leading to a significant improvement in prefilling efficiency. (i) For 100k token contexts prefilling, the attention layer achieves a 7.47x speedup, while the end-to-end 2.58x speedup without compromising generation quality. This highlights the practical viability and superiority of PEVLM in cloud deployment scenarios. (ii) Under fixed latency constraints, PEVLM increases accuracy from 23.26% to 61.03%, showcasing its critical value for latency sensitive applications.

Observations

To explore the application of parallel encoding in VLMs, we analyzed the potential differences between LLMs and VLMs that may affect accuracy:

(i) **In VLMs, attention sinks are present not only in the initial system prompt, but also in the early video frames** (Kang et al. 2025). To achieve optimal performance, it may be necessary to include enough frames in the sink.

(ii) Existing parallel-encoding-based methods are primarily designed for Retrieval-Augmented Generation (RAG) tasks (Ma, Wang, and Tian 2025; Yang, Chen, and Chen 2025; Lu et al. 2024). In such tasks, reusing the KV cache from previously retrieved passages is crucial for enhancing inference efficiency. Since the order of passages often changes when reusing the KV cache, a common strategy is to apply parallel encoding to generate the KV cache for each passage independently, while sharing position embeddings across passages, as illustrated in Figure 3. As a result, position embeddings are typically shared across blocks. However, **preserving the correct temporal order of video frames is critical for video understanding tasks**. Blindly reusing position embeddings across blocks can disrupt the model’s ability to capture temporal dependencies. This disruption is especially severe for models where the temporal component of the position embeddings is explicitly aligned with absolute time (Bai et al. 2025).

Therefore, as illustrated in Figure 1, we perform an attention weight analysis for VLMs and make two key findings:

(i) As shown in Figure 1(a), initial segments of both text and video receive high attention weights, emphasizing the need to include early video frames when selecting sink tokens.

(ii) As shown in Figure 1(b), compared to Full-Attention, the initial video frames receive even higher attention weights, while the remaining frames exhibit more uniform and lower attention weights. In contrast, when sequential position embeddings are preserved, as illustrated in Figure 1(c), parallel encoding yields an attention score distribution that more closely resembles that of Full-Attention.

These observations yield two key insights for applying parallel encoding to VLMs: The shared sink block in parallel encoding should include early video frames in addition to textual prompts, as they function as important attention sinks. Maintaining the sequential position embeddings of video tokens is essential for preserving temporal consistency; reusing position embeddings across blocks can disrupt temporal alignment. These findings underscore the need for a

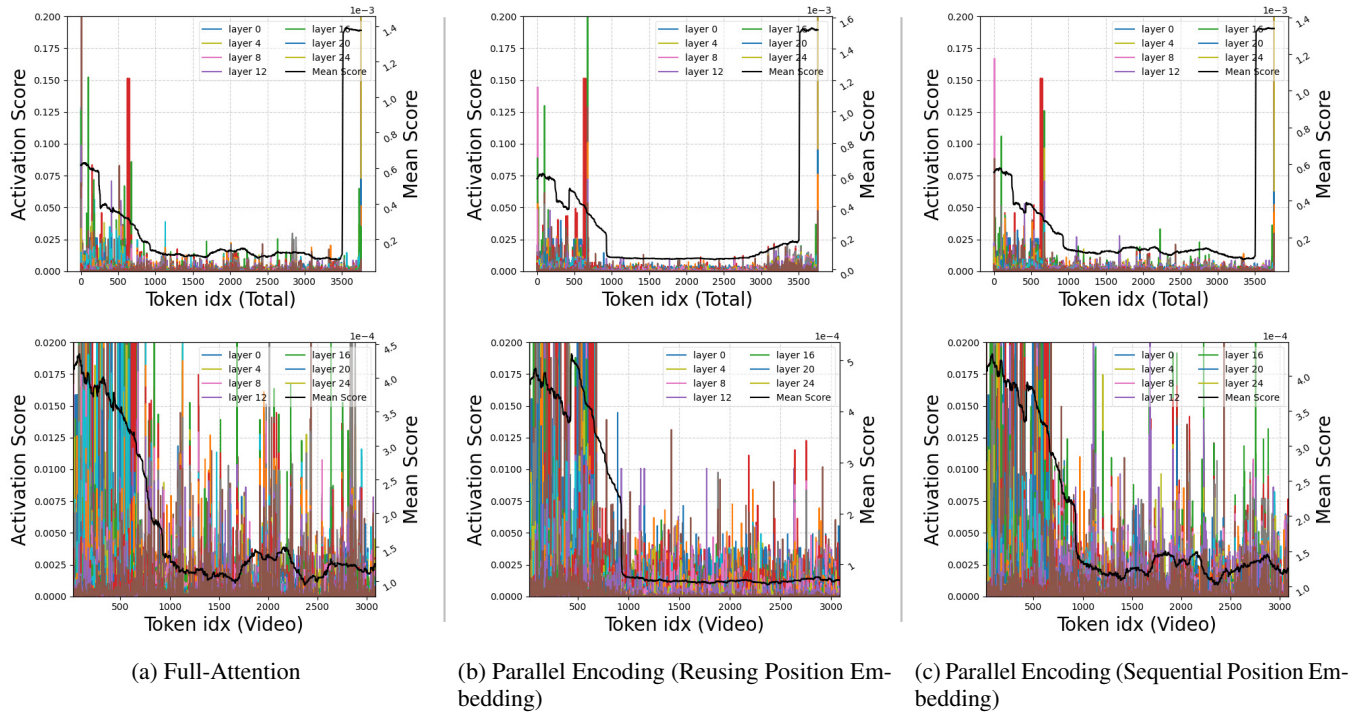


Figure 1: We collected the distribution of attention weights under different scenarios and computed their moving averages for better observation. The top row shows the attention weights for all tokens, while the bottom row shows those for the video tokens. (a) Full-Attention: The textual tokens and the initial video frames receive the highest attention weights, whereas the remaining video frames are assigned relatively lower attention weights. (b) Parallel Encoding (Reusing Position Embedding): The overall attention weights distribution resembles Full-Attention, with higher attention weights for the textual tokens and initial video frames. While compared to Full-Attention, the initial video frames receive even higher attention weights, and the remaining video frames exhibit more uniform and lower attention weights. (c) Parallel Encoding (Sequential Position Embedding): The overall attention weights distribution remains similar to (a) and (b). However, the attention weight distribution within the video frames more closely aligns with (a).

VLM-specific parallel encoding strategy, which we introduce in the next section.

PEVLM

With the observation in the last section, we design PEVLM to improve computational efficiency. PEVLM enables a seamless shift to parallel encoding without requiring training while maintaining most of the model’s capabilities. Our approach adaptively aligns the distribution of attention weights between Full-Attention and parallel encoding, thereby boosting efficiency and performance.

Standard Attention Mechanism

In a standard Softmax attention, we attend the query to all past KV states using the following formula:

$$O = \text{Softmax}\left(\frac{QK^T}{\sqrt{d}}\right)V \quad Q \in \mathbb{R}^{n \times d} \quad K, V \in \mathbb{R}^{m \times d} \quad (1)$$

where Q is the query state, and K and V denote the key and value states, respectively.

Attention Sink. First discovered by StreamingLLM (Lab and AI 2023), that one or more tokens at the start position of

an LLM receive higher attention scores. APE (Yang, Chen, and Chen 2025) and Star-Attention (Liu et al. 2024) have demonstrated that sharing a common attention sink across parallel encoding blocks significantly enhances model accuracy. Some VLM-related studies also show that the attention sink phenomenon exists in VLMs but is more distributed among image tokens (Kang et al. 2025).

Position Embedding. To effectively process sequential input, LLMs require position embeddings, such as absolute position embeddings (Devlin et al. 2019; Vaswani et al. 2017) and relative position embeddings (Press, Smith, and Lewis 2022; Su et al. 2024). For VLMs, contextual positional information is more critical. In particular, for some VLM models like Qwen2.5-VL, their position embeddings also incorporate spatio-temporal information between video frames, making position embeddings increasingly essential for VLMs.

Computational Complexity. In standard softmax attention mechanisms, the total number of operations is given by

$$OP_{Attn} = 2HL^2, \quad (2)$$

where L is the context length and H is the hidden size. This leads to a computational complexity of $O(L^2)$. As L in-

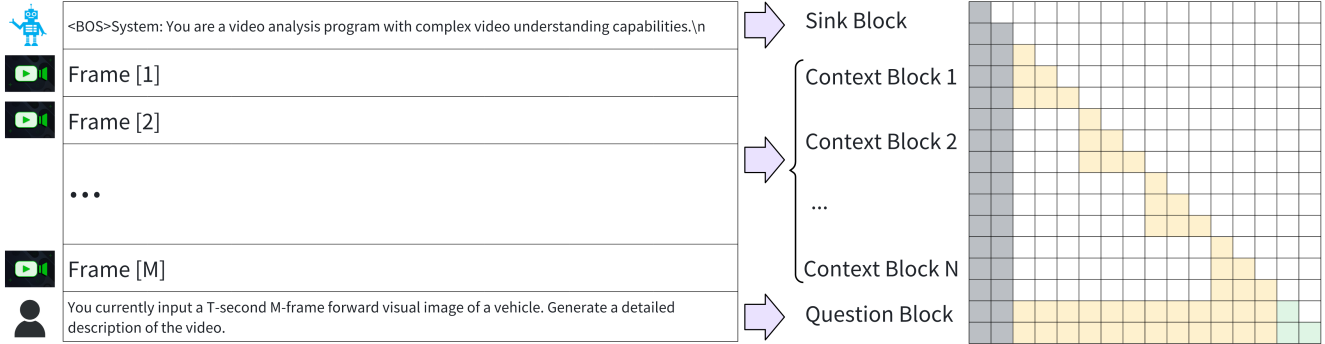


Figure 2: The PEVLM Masks.

creases, the cost grows quadratically, severely limiting the speed and scalability of the inference. This issue is further exacerbated in VLMs. For a video consisting of T frames, where each frame is represented by N tokens (typically ranging from hundreds to thousands), the total context length becomes $L = T \times N$, resulting in a complexity of $O((T \times N)^2)$. Such scaling renders standard attention mechanisms impractical for long-video understanding tasks.

Parallel Encoding

Partitioning Strategy As illustrated in Figure 2, our partitioning strategy consists of three core components:

- **Sink Block:** The initial text tokens (e.g., BOS token and system prompts) and the first several video frames are grouped into a dedicated Sink Block.
- **Context Blocks:** The remaining video content is uniformly partitioned into Context Blocks by frames to reduce computational overhead and enable parallelization.
- **Question Block:** The text tokens that follow the video input are left unsegmented as Question Block.

Since the information within each video frame represents spatial content at a specific moment, while information across frames reflects temporal dynamics, videos naturally possess structural boundaries. If the video are divided into sink and context blocks by token count, this may compromise the spatial integrity of the boundary frames shared between adjacent blocks. So we divide the video by frame.

Sink Size & Block Size In addition, as analyzed in the last section, the number of frames selected for the Sink Block depends primarily on the distribution of attention weights. The optimal strategy is to include all tokens with significantly higher attention scores at the beginning of the video in the Sink Block. However, as shown in Equation 11, a larger sink size results in higher latency, leading to a trade-off between accuracy and efficiency. A similar trade-off also arises in the selection of block size.

Formulations For different blocks, PEVLM applies distinct computation methods to ensure efficient processing and

information integration:

$$\text{Attn}_s = f(Q_s, K_s, V_s), \quad (3)$$

$$\text{Attn}_{c_i} = f(Q_{c_i}, K_{s+c_0+\dots+c_{i-1}}, V_{s+c_0+\dots+c_{i-1}}), \quad (4)$$

$$\text{Attn}_q = f(Q_q, K_{s+c_{\text{all}}+q}, V_{s+c_{\text{all}}+q}), \quad (5)$$

where s and q are the Sink Block and question block, c_i is the i th Context Blocks; Attn_s , Attn_{c_i} and Attn_q denote the attention of the s , c_i and q . $f(\cdot)$ represents the standard Softmax attention in Equation (1), and Q , K and V denote the query, key, and value matrices.

The total OP of PEVLM is

$$OP_{\text{PEVLM}} = OP_{\text{Sink}} + N \times OP_{\text{ContextBlock}} + OP_{\text{Quest}}, \quad (6)$$

$$OP_{\text{Sink}} = 2HS^2, \quad (7)$$

$$OP_{\text{ContextBlock}} = 2HB(S + B), \quad (8)$$

$$OP_{\text{Quest}} = 2HQL, \quad (9)$$

where S denotes the sink size, N denotes the block number, B denotes the block size, Q denotes the query size and H is the hidden size. L is the total token number and $L = S + N \times B + Q$.

After simplification:

$$OP_{\text{PEVLM}} = 2H(S^2 + Q^2 + NB^2) \quad (10)$$

$$+ QS + NQB + NSB). \quad (11)$$

As the block size is a static number, the computational complexity of PEVLM is $O(L)$.

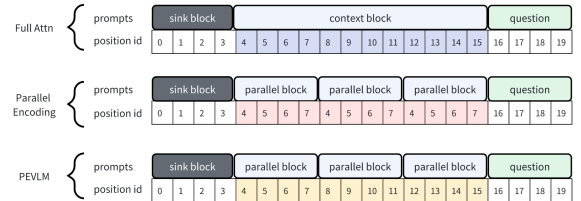


Figure 3: Position Encoding in PEVLM

Position Encoding As described in observations, similar to the case in LLMs, applying parallel-encoding-based methods

Table 1: Performance (\uparrow) of different models and different methods on video understanding tasks evaluated at tokens from 26k to 100k.

| Model | Method | MVBench | EgoSchema | VideoMME | | LongVideoBench | |
|---|-------------|---------------|----------------|---------------|---------------|----------------|---------------|
| | | 17s in avg. | 3 mins in avg. | < 2mins | [2mins, 1h] | < 1min | [1min, 1h] |
| Qwen2.5-VL- 7B-Instruct <i>Max pixels: 90M</i> <i>Tokens: 100k</i> | Full Attn | 68.47% | 57.00% | 74.56% | 56.72% | 72.85% | 55.33% |
| | Block Attn | 66.03% | 47.40% | 65.22% | 50.39% | 70.64% | 47.85% |
| | APE (T=1.0) | 66.03% | 57.20% | 50.56% | 1.06% | 54.02% | 3.38% |
| | Star Attn | 60.19% | 19.80% | 3.00% | 0.00% | 49.03% | 0.00% |
| | PEVLM | 68.44% | 61.00% | 74.33% | 58.83% | 74.52% | 57.58% |
| LongVILA- 7B-256f <i>Frames: 256</i> <i>Tokens: 66k</i> | Full Attn | 61.92% | 57.00% | 66.33% | 49.39% | 65.10% | 47.44% |
| | Block Attn | 57.81% | 59.00% | 64.89% | 51.44% | 61.77% | 48.05% |
| | APE (T=1.0) | 60.00% | 60.60% | 68.56% | 51.61% | 63.71% | 46.93% |
| | Star Attn | 63.39% | 61.60% | 70.11% | 54.17% | 63.43% | 47.44% |
| | PEVLM | 63.53% | 61.40% | 69.44% | 54.33% | 65.93% | 49.18% |
| LLaVA-Video- 7B-Qwen2 (128) <i>Frames: 128</i> <i>Tokens: 26k</i> | Full Attn | 60.67% | 58.20% | 75.33% | 59.99% | 72.02% | 55.53% |
| | Block Attn | 56.86% | 51.60% | 67.56% | 55.50% | 63.99% | 52.36% |
| | APE (T=1.0) | 58.00% | 57.60% | 72.22% | 58.19% | 67.87% | 54.61% |
| | Star Attn | 59.31% | 57.80% | 72.89% | 58.71% | 68.98% | 54.92% |
| | PEVLM | 60.00% | 58.20% | 74.33% | 59.99% | 72.02% | 55.53% |

in VLMs suffers from the misalignment of attention weight distributions when compared to Full-Attention. However, introducing additional hyperparameters to adjust attention weights for better alignment is not ideal for efficient deployment. Therefore, inspired by Block Attention (Ma, Wang, and Tian 2025) and TurboRAG (Lu et al. 2024), we retain sequential position embeddings as illustrated in Figure 3.

Due to retaining the sequential position embeddings, PEVLM does not extend the model’s inherent capacity to handle longer video contexts, unlike some other parallel encoding-based approaches. For instance, LongVILA-7B-256f is generally trained to process up to 256 frames, and feeding longer videos may lead to accuracy degradation. Although PEVLM accelerates inference, it still processes 256 frames, and longer inputs may still result in degraded performance. However, this is acceptable, as our primary objective is to improve prefilling efficiency.

Experiments

In this section, we test PEVLM from multiple perspectives against several different VLMs. The primary objective is to evaluate the accuracy, computational efficiency, and real-world applicability of PEVLM for long-video processing. And to better reflect practical deployment scenarios, we designed the experiments from two perspectives. (i) We first test with workloads of approximately 100k tokens to assess the acceleration performance of PEVLM in cloud serving platforms. (ii) Furthermore, we evaluate PEVLM on the LongVideoBench dataset under a given latency constraint, in order to measure its effectiveness in edge scenarios where both computational resources and latency are limited.

Accuracy Evaluation

Setup The main objective of this experiment is to analyze the impact of PEVLM on accuracy in long-video understand-

ing tasks. We have chosen the LongVideoBench (Zhang and Wang 2024), VideoMME (Fu et al. 2024), EgoSchema (Mangalam, Akshulakov, and Malik 2023), and MVBench (Li et al. 2024a) as benchmarks, which are designed to comprehensively evaluate multimodal models in video understanding. We have carried out experiments using LLaVA-Video (Zhang et al. 2024), LongVILA (Chen et al. 2024), and Qwen2.5-VL (Bai et al. 2025) as test models. To minimize any adverse effects on accuracy, all evaluations were performed using bf16 precision.

As shown in Table 1, we compared the accuracy of Full-Attention, Block-Attention, APE, Star-Attention, and PEVLM in the datasets. Since the other methods are finetune-free, we did not finetune the weights in the Block Attention test. For APE, to accommodate the needs of large-scale deployment, we tested with T=0. Regarding the sink block (shared prefix), we selected the system prompt by referring to the code provided by APE. For Star-Attention, we implemented its equivalent algorithm on a single node, with the anchor size set equal to the block size, as the configuration in the Block-Attention paper (Ma, Wang, and Tian 2025). The block size was uniformly set to 4096 across all algorithms. Smaller block sizes resulted in reduced accuracy for all methods, while larger blocks significantly degraded inference performance. For PEVLM, we set the sink size and block size to about 16 frames, which corresponds to approximately 4k tokens for Qwen2.5-VL and LongVILA, and about 3k tokens for LLaVA-Video.

Results The experiments show that PEVLM achieves an accuracy comparable to, and in some cases even surpassing, that of Full-Attention across all three evaluated models. Both APE and Star-Attention also approach or exceed the accuracy of Full-Attention when Full-Attention’s position encoding is retained. However, Block-Attention exhibits a notable accuracy drop compared to Full-Attention in most settings,

primarily due to the lack of alignment-specific fine-tuning.

Although parallel encoding is generally expected to degrade performance, it can instead improve accuracy in long-context scenarios. This is because parallel encoding effectively shortens the total token length involved in each softmax computation, thereby mitigating the softmax feature degradation that occurs with long contexts (Veličković et al. 2025). As a result, the softmax output more robustly approximates an ideal sharp function, which ultimately enhances the performance of some models under long-context conditions.

Performance Evaluation

In this section, we evaluate the performance of PEVLM. To facilitate experimentation, we built PEVLM basied on the SGLang, which is a fast serving framework for large language models and vision-language models, widely used in cloud production deployment.

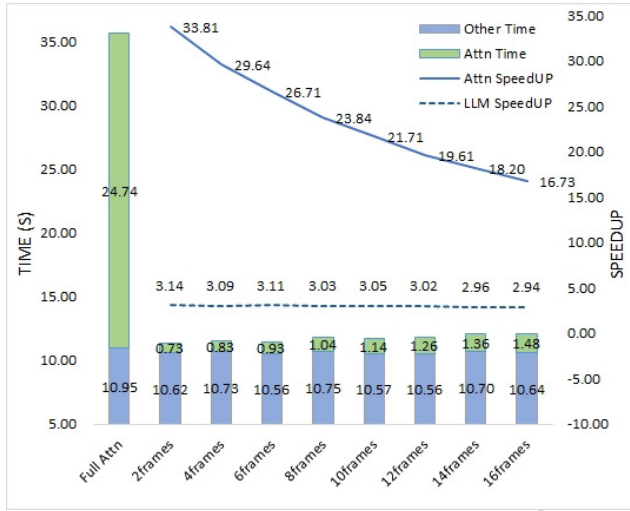


Figure 4: We evaluate PEVLM under different block_size settings. The sink_size is set to (system prompt+one frame). "Attn Time" refers to attention computation time, and "Other Time" covers all other LLM costs. "Attn SpeedUP" and "LLM SpeedUP" indicate the acceleration over Attention layer and overall LLM performance.

Setup Since the LLM component in VLM models remains largely consistent across different implementations, performance differences arise primarily from hyperparameter configurations rather than model weights. Consequently, we conducted computational efficiency evaluations on the Qwen2.5-VL model. The primary objective of this experiment is to assess the improvements in computational efficiency introduced by PEVLM. All experiments were carried out on an NVIDIA H20-96G GPGPU. Given that PEVLM primarily optimizes the attention mechanism within the LLM, we measured the execution time of both the entire LLM module and its individual attention layers separately.

Results As illustrated in Figure 4 and Figure 5, the end-to-end inference speed of the LLM is improved by 2.58 \times

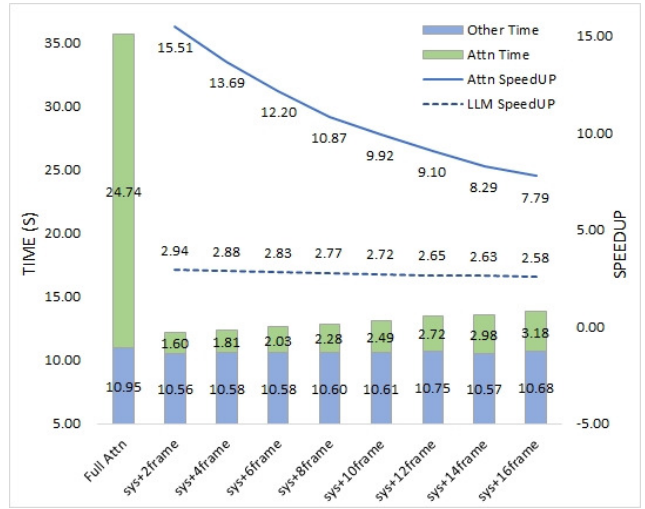


Figure 5: We evaluate PEVLM under different sink_size settings. The block_size is set to (16 frames). "Attn Time" refers to attention computation time, and "Other Time" covers all other LLM costs. "Attn SpeedUP" and "LLM SpeedUP" indicate the acceleration over Attention layer and overall LLM performance.

to 3.14 \times . Notably, the attention module achieves a speedup ranging from 7.79 \times to 33.81 \times , while the execution time of non-attention components remains largely unaffected. As the block size or sink size increases, the acceleration effect of the attention module decreases significantly. This observation is consistent with the Equation 11. Moreover, because non-attention components constitute a substantial portion of the total runtime in PEVLM, the overall end-to-end speedup of the LLM moderately decreases from 3.14 \times to 2.58 \times .

Accuracy with Limited Latency

One key challenge in deploying VLMs on edge devices is the limited computational resources and strict latency requirements. To evaluate the acceleration performance of PEVLM under this scenario, we designed a simulation accordingly. A simplified experimental setup was implemented to assess the efficiency of PEVLM in edge deployment settings.

Table 2: Accuracy with Limited Latency

| | Full Attn | Full Attn (3B) | PEVLM | |
|----------|-----------|----------------|---------------|---------------|
| | sink | block | sys+2f | sys+16f |
| No Limit | 60.43% | 55.05% | 61.18% | 62.23% |
| 40s | 59.69% | 55.05% | 61.18% | 62.23% |
| 30s | 27.08% | 55.05% | 61.18% | 62.23% |
| 20s | 23.26% | 24.38% | 61.03% | 60.28% |

Setup We use LongVideoBench as the evaluation benchmark and introduce a latency constraint during inference:

any sample whose inference time exceeds the predefined latency threshold is considered a failure. The experiments are conducted on the H20-96B platform. We select Qwen2.5-VL-7B-Instruct with Full-Attention as the baseline, and compare Full-Attention, PEVLM, and using smaller models (Qwen2.5-VL-3B-Instruct).

Results As shown in Table 2, the accuracy of Full-Attention drops significantly when the latency constraint is reduced from 40s to 30s, while the accuracy of Full-Attention 3B also declines sharply when the latency constraint is tightened from 30s to 20s. PEVLM maintain relatively high accuracy even at 20s. Notably, although larger sink and block sizes (e.g., sys+16frames, block=16frames) achieve higher accuracy under looser latency constraints, the smaller sink size (sink=sys+2frames, block=16frames) delivers better accuracy at the 20s latency limit due to its lower latency.

How does each component in PEVLM contribute to the performance?

In Table 3, we present an ablation study to evaluate the contribution of each component in PEVLM, including the use of Sequential Position Embedding (SP), Dividing the Video by Frames (DF), and Adding Frames to the Sink (FS). The results are averaged across the four base models reported in Table 1. We observe that sequential parallel encoding yields the most significant improvement in accuracy, achieving an average performance gain of 12.64%. Incorporating the initial frames into the sink block leads to an additional average accuracy gain of 1.54%. In contrast, dividing the video by frames provides only a marginal improvement compared to directly segmenting the video without this strategy.

Table 3: Ablation study of PEVLM components on LongVideoBench

| SP | DF | FS | LongVideoBench | VideoMME |
|----|----|----|----------------|----------|
| ✓ | | | 46.67% | 45.31% |
| ✓ | ✓ | | 56.75% | 60.51% |
| ✓ | ✓ | ✓ | 56.77% | 60.63% |
| | | | 58.26% | 62.22% |

Position Encoding

We further analyze the component with the greatest impact on accuracy: the use of sequential position embeddings. As discussed before, adopting sequential position embeddings instead of reusing position embeddings across blocks produces attention distributions that more closely resemble those of Full-Attention, thereby aligning better with the model’s expected behavior. As shown in Table 4, the use of sequential position embeddings significantly improves accuracy in both Qwen2.5-VL and LongVILA. In contrast, for the LLaVA-Video model, the benefit is marginal, likely because its attention weight distribution (as shown in Figure 9 in the Appendix) remains relatively stable even when using parallel encoding.

Table 4: Accuracy \uparrow on LongVideoBench dataset with Different Position Embedding Strategy

| model | method | reuse pos | sequential |
|----------------------------|-------------|-----------|------------|
| Qwen2.5-VL-7B-Instruct | APE (T=1.0) | 30.44% | 59.39% |
| | Star Attn | 29.54% | 61.41% |
| | PEVLM | 14.73% | 62.23% |
| 7B-256f | APE (T=1.0) | 51.46% | 53.40% |
| | Star Attn | 51.76% | 53.63% |
| | PEVLM | 49.96% | 53.70% |
| LLaVA-Video-7B-Qwen2 (128) | APE (T=1.0) | 58.19% | 58.12% |
| | Star Attn | 58.71% | 58.49% |
| | PEVLM | 58.34% | 59.01% |

Sink & Block Size

As analyzed in the third section, the inference latency of PEVLM increases quadratically with the sink size, which is consistent with the experimental results shown in Figure 5.

Furthermore, we investigate the impact of sink size on model accuracy. As observed in the second section, it is essential to involve the initial frames of the video in the sink. This observation is validated in Figure 6, where incorporating the initial frames into the sink leads to varying degrees of accuracy improvement across different models.

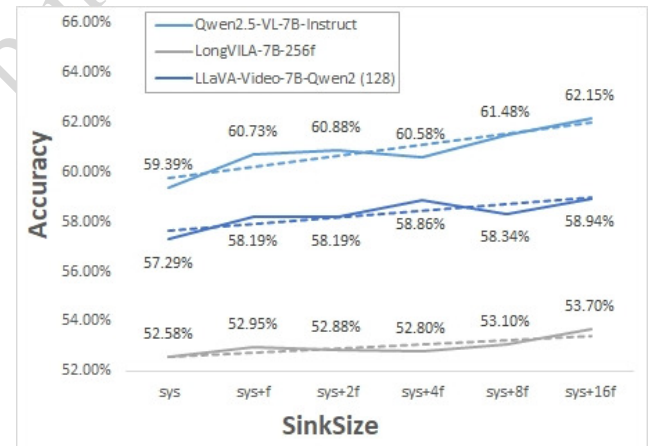


Figure 6: The impact of sink sizes on accuracy

Moreover, as shown in Figure 6, the accuracy of all models shows an upward trend as the sink size increases. However, because of the quadratic increase in latency, using longer sink sizes is not favorable for performance. Therefore, it may be necessary to conduct a simple test prior to deployment to determine an appropriate sink size. For the three models shown in Figure 6, setting the sink size between 14 and 18 already yields strong accuracy. If latency constraints are also taken into account, this could lead to a trade-off between performance and accuracy. For example, as demonstrated in the results of Table 2, under a 20-second latency constraint, using only sys+2frames as the Sink Block achieves better accuracy than using sys+16frames.

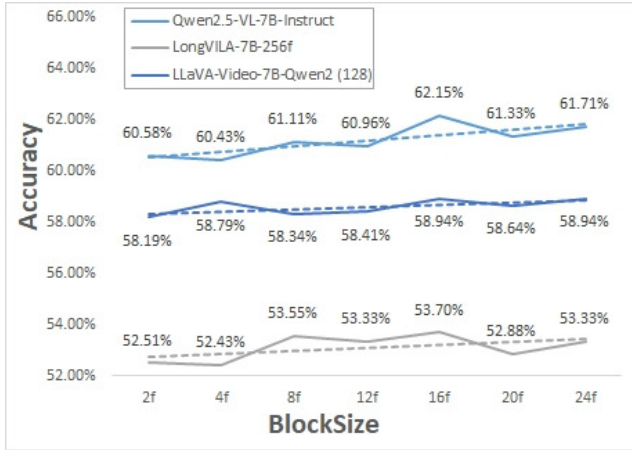


Figure 7: The impact of block sizes on accuracy

As shown in Figure 4, the inference latency of PEVLM also increases quadratically with block size, which is consistent with the experimental results shown in Figure 4. However, the block size has a more significant impact on performance because the coefficient of the block size’s quadratic term in Equation 11 is much larger than that of the sink size.

We investigate the impact of block size on model accuracy here. As shown in Figure 7, the model accuracy exhibits an upward trend as the block size increases, similar to sink size. However, due to the quadratic growth in latency, a trade-off arises between computational efficiency and accuracy.

Conclusion

This study investigates the potential of parallel-encoding-based methods in VLMs, which can reduce the computational complexity of attention mechanisms for fast inference and reuse positions for long-context processing but often result in performance degradation. To address this issue, we propose PEVLM, a training-free method designed to enable accurate, fast, and long-context video processing. PEVLM achieves this by aligning the attention weight distribution of parallel encoding with Full-Attention through two key steps: selecting an appropriate sink size and block size, and utilizing sequential position embeddings. Empirically, we demonstrate that PEVLM enhances both accuracy and efficiency in long video processing tasks while successfully scaling to process hundreds of chunks in parallel across various settings.

Future Work

Although PEVLM has demonstrated substantial improvements in computational efficiency and reasoning performance for long video processing tasks, there remains ample opportunity for further research and enhancement. In future work, we plan to explore the following directions.

Beyond video inputs, an important future direction is extending PEVLM to handle richer multimodal inputs such as LiDAR, map priors, and inertial measurements, which are commonly used in domains like autonomous driving and robotics. These modalities often exhibit different spatial and

temporal characteristics compared to visual tokens, posing unique alignment and fusion challenges for attention-based models. Enhancing PEVLM with cross-modal position encoding strategies and adaptive sink block selection could further improve its generalization to complex, heterogeneous input streams.

One promising direction is extending PEVLM to streaming or online scenarios, such as autonomous driving, where the model continuously receives multimodal inputs (e.g., video frames and LiDAR) over time. In these settings, a fixed-length sliding temporal window is often adopted: new data is appended while the oldest is discarded, maintaining a constant context size that reflects the most recent few seconds or minutes of input. If PEVLM can be adapted to such settings, it would allow the model to compute only over the newly arrived data at each inference step, rather than reprocessing the entire history. This could lead to significant performance gains—potentially improving inference speed by several times or even orders of magnitude. Such an extension would enable real-time video-language reasoning under strict latency constraints and dynamic, continuously evolving environments.

References

Alayrac, J. B.; et al. 2022. Flamingo: A Visual Language Model for Few-Shot Learning. *arXiv preprint*.

Bai, S.; Chen, K.; Liu, X.; Wang, J.; Ge, W.; Song, S.; Dang, K.; Wang, P.; Wang, S.; Tang, J.; Zhong, H.; Zhu, Y.; Yang, M.; Li, Z.; Wan, J.; Wang, P.; Ding, W.; Fu, Z.; Xu, Y.; Ye, J.; Zhang, X.; Xie, T.; Cheng, Z.; Zhang, H.; Yang, Z.; Xu, H.; and Lin, J. 2025. Qwen2.5-VL Technical Report. arXiv:2502.13923.

Beltagy, I.; Peters, M. E.; and Cohan, A. 2020. Longformer: The Long-Document Transformer. *arXiv preprint*.

Black, M.; Lee, K.; et al. 2024. Humanoid robots learn from multimodal web data with VLMs. *arXiv preprint arXiv:2403.00001*.

Cheang, L.; Huang, X.; et al. 2024. Robot Agents with Long-Horizon Multimodal Memory. *arXiv preprint arXiv:2402.01234*.

Chen, Y.; Xue, F.; Li, D.; Hu, Q.; Zhu, L.; Li, X.; Fang, Y.; Tang, H.; Yang, S.; Liu, Z.; He, E.; Yin, H.; Molchanov, P.; Kautz, J.; Fan, L.; Zhu, Y.; Lu, Y.; and Han, S. 2024. LongVILA: Scaling Long-Context Visual Language Models for Long Videos. arXiv:2408.10188.

Devlin, J.; Chang, M.-W.; Lee, K.; and Toutanova, K. 2019. BERT: Pre-training of Deep Bidirectional Transformers for Language Understanding. In Burstein, J.; Doran, C.; and Solorio, T., eds., *Proceedings of the 2019 Conference of the North American Chapter of the Association for Computational Linguistics: Human Language Technologies, Volume 1 (Long and Short Papers)*, 4171–4186. Minneapolis, Minnesota: Association for Computational Linguistics.

Fu, C.; Dai, Y.; Luo, Y.; Li, L.; Ren, S.; Zhang, R.; Wang, Z.; Zhou, C.; Shen, Y.; Zhang, M.; et al. 2024. Video-MME: The First-Ever Comprehensive Evaluation Benchmark of Multi-modal LLMs in Video Analysis. *arXiv preprint arXiv:2405.21075*.

Gao, L.; Lin, C.; et al. 2024. Perception and Planning with Long Context VLMs. *arXiv preprint arXiv:2403.07698*.

Guu, K.; et al. 2020. Retrieval-Augmented Language Model Pretraining. In *ICML*.

Hu, Y.; Wu, Z.; et al. 2023. DriveVLM: Adaptive Vision-Language Modeling for Autonomous Driving. *arXiv preprint arXiv:2311.09876*.

Kang, S.; Kim, J.; Kim, J.; and Hwang, S. J. 2025. See What You Are Told: Visual Attention Sink in Large Multimodal Models. *arXiv:2503.03321*.

Lab, M.-H.; and AI, M. 2023. StreamingLLM: Enabling Infinite-Length Generation with Attention Sinks. *arXiv preprint arXiv:2309.17453*.

Li, K.; Wang, Y.; He, Y.; Li, Y.; Wang, Y.; Liu, Y.; Wang, Z.; Xu, J.; Chen, G.; Luo, P.; Wang, L.; and Qiao, Y. 2024a. MVBench: A Comprehensive Multi-modal Video Understanding Benchmark. *arXiv:2311.17005*.

Li, X.; Yin, X.; Li, C.; Hu, X.; Zhang, P.; Zhang, L.; Wang, L.; Hu, H.; Dong, L.; Wei, F.; et al. 2020. Oscar: Object-semantics aligned pre-training for vision-language tasks. In *ECCV*.

Li, Z.; Zhang, Y.; Pan, T.; Sun, Y.; Duan, Z.; Fang, J.; Han, R.; Wang, Z.; and Wang, J. 2024b. FocusLLM: Precise Understanding of Long Context by Dynamic Condensing. *arXiv:2408.11745*.

Liu, N. F.; Lin, K.; Hewitt, J.; Paranjape, A.; Bevilacqua, M.; Petroni, F.; and Liang, P. 2023. Lost in the Middle: How Language Models Use Long Contexts. *Transactions of the Association for Computational Linguistics*, 12: 157–173.

Liu, X.; Zhang, W.; et al. 2024. BMed-VL: A Vision-Language Model for Multimodal Biomedical Reasoning. *arXiv preprint arXiv:2401.04512*.

Liu, Y.; et al. 2024. Star Attention: Sparse Approximation Strategies for Efficient Long-Context Modeling. *arXiv preprint*.

Lu, E.; Jiang, Z.; Liu, J.; Du, Y.; Jiang, T.; Hong, C.; Liu, S.; He, W.; Yuan, E.; Wang, Y.; Huang, Z.; Yuan, H.; Xu, S.; Xu, X.; Lai, G.; Chen, Y.; Zheng, H.; Yan, J.; Su, J.; Wu, Y.; Zhang, N. Y.; Yang, Z.; Zhou, X.; Zhang, M.; and Qiu, J. 2025. MoBA: Mixture of Block Attention for Long-Context LLMs. *arXiv:2502.13189*.

Lu, S.; Wang, H.; Rong, Y.; Chen, Z.; and Tang, Y. 2024. TurboRAG: Accelerating Retrieval-Augmented Generation with Precomputed KV Caches for Chunked Text. *arXiv:2410.07590*.

Ma, D.; Wang, Y.; and Tian, L. 2025. Block-Attention for Efficient Prefilling. *arXiv:2409.15355*.

Mangalam, K.; Akshulakov, R.; and Malik, J. 2023. EgoSchema: A Diagnostic Benchmark for Very Long-form Video Language Understanding. In Oh, A.; Naumann, T.; Globerson, A.; Saenko, K.; Hardt, M.; and Levine, S., eds., *Advances in Neural Information Processing Systems*, volume 36, 46212–46244. Curran Associates, Inc.

Prasad, R.; Singh, A.; et al. 2024. Embodied VLMs for instruction following in robotics. In *Proceedings of the IEEE/CVF Conference on Computer Vision and Pattern Recognition (CVPR)*.

Press, O.; Smith, N. A.; and Lewis, M. 2022. Train Short, Test Long: Attention with Linear Biases Enables Input Length Extrapolation. *arXiv:2108.12409*.

Radford, A.; et al. 2021. Learning Transferable Visual Models From Natural Language Supervision. In *ICML*.

Ratner, N.; Levine, Y.; Belinkov, Y.; Ram, O.; Magar, I.; Abend, O.; Karpas, E.; Shashua, A.; Leyton-Brown, K.; and Shoham, Y. 2023. Parallel Context Windows for Large Language Models. *arXiv:2212.10947*.

Su, J.; Ahmed, M.; Lu, Y.; Pan, S.; Bo, W.; and Liu, Y. 2024. RoFormer: Enhanced transformer with Rotary Position Embedding. *Neurocomputing*, 568: 127063.

Vaswani, A.; et al. 2017. Attention is All You Need. In *NeurIPS*.

Veličković, P.; Perivolaropoulos, C.; Barbero, F.; and Pascanu, R. 2025. Softmax is not Enough (for Sharp Size Generalisation). *arXiv:2410.01104*.

Wang, M.; Zhao, T.; et al. 2024. Cascaded Multimodal Transformers for Driving Video Analysis. *arXiv preprint arXiv:2401.05678*.

Yang, X.; Chen, T.; and Chen, B. 2025. APE: Faster and Longer Context-Augmented Generation via Adaptive Parallel Encoding. In *The Thirteenth International Conference on Learning Representations*.

Yen, H.; Gao, T.; and Chen, D. 2024. Long-Context Language Modeling with Parallel Context Encoding. *arXiv:2402.16617*.

Yuan, J.; Gao, H.; Dai, D.; Luo, J.; Zhao, L.; Zhang, Z.; Xie, Z.; Wei, Y. X.; Wang, L.; Xiao, Z.; Wang, Y.; Ruan, C.; Zhang, M.; Liang, W.; and Zeng, W. 2025. Native Sparse Attention: Hardware-Aligned and Natively Trainable Sparse Attention. *arXiv:2502.11089*.

Zhang, T.; and Wang, K. 2024. LongVideoBench: Evaluating long video understanding for VLMs. In *Conference on Neural Information Processing Systems (NeurIPS)*.

Zhang, Y.; Wu, J.; Li, W.; Li, B.; Ma, Z.; Liu, Z.; and Li, C. 2024. Video Instruction Tuning With Synthetic Data. *arXiv:2410.02713*.

Zhu, D.; Ding, X.; Wang, J.; Yang, L.; and Hu, X. 2023. MiniGPT-4: Enhancing Vision-Language Understanding with GPT-4 Level Capabilities. *arXiv preprint arXiv:2304.10592*.

Benchmark Details

We evaluate our method on several video understanding benchmarks that test different aspects of video comprehension:

EgoSchema

EgoSchema (Mangalam, Akshulakov, and Malik 2023) is a large-scale benchmark designed to evaluate Multimodal Large Language Models (MLLMs) on egocentric video understanding. It consists of 100 hours of first-person video data spanning 1,270 daily activity episodes across diverse real-world environments. The benchmark introduces over 10,000 manually curated question-answer pairs, covering tasks such as object grounding, human-object interaction, activity reasoning, and intent prediction.

MVBench

MVBench (Li et al. 2024a) is a comprehensive benchmark designed to evaluate Multimodal Large Language Models (MLLMs) on multi-granular video understanding. It consists of 5 task categories—including moment-level, frame-level, clip-level, video-level, and holistic video understanding—covering a wide range of temporal scopes and reasoning demands. The benchmark includes 2,562 manually annotated questions grounded in 4,119 diverse video clips, selected from real-world scenarios.

Each question is carefully designed to probe different levels of spatiotemporal understanding, from fine-grained object recognition and short-term motion tracking to long-term event inference. MVBench offers a unified and challenging evaluation protocol to assess the generalization and reasoning ability of MLLMs across granularities.

Unlike conventional third-person video datasets, EgoSchema emphasizes embodied perception and temporal reasoning from an egocentric perspective, posing unique challenges for spatial understanding, long-term memory, and causal inference in MLLMs.

Video-MME

Video-MME (Fu et al. 2024) is a comprehensive evaluation benchmark for assessing the video understanding capabilities of Multimodal Large Language Models (MLLMs). It spans 6 primary visual domains and 30 subfields, covering a diverse range of video types and temporal scenarios. The benchmark includes 900 videos with durations ranging from 11 seconds to 1 hour, totaling 254 hours of content.

To evaluate fine-grained visual and temporal reasoning, 2,700 manually annotated question-answer pairs are provided. Video-MME challenges models to comprehend both short and long video clips across different temporal granularities, making it a rigorous benchmark for evaluating the core video processing capabilities of MLLMs.

LongVideoBench

LongVideoBench (Zhang and Wang 2024) is a benchmark specifically designed to evaluate the long-context video understanding capabilities of Multimodal Large Language Models (MLLMs). It features 1,760 videos spanning 12 diverse real-world scenarios, with video durations ranging from 5 minutes to 2 hours, totaling over 1,000 hours of content. The benchmark includes 2,400 manually annotated multi-choice questions targeting key aspects of long video comprehension.

LongVideoBench focuses on challenging long-range temporal reasoning, event tracking, and global understanding across extended video content. It aims to assess whether models can maintain coherence, memory, and attention over prolonged contexts, making it a rigorous testbed for long-form video modeling.

Attention Weights Distribution of LLaVA-Video and LongVILA

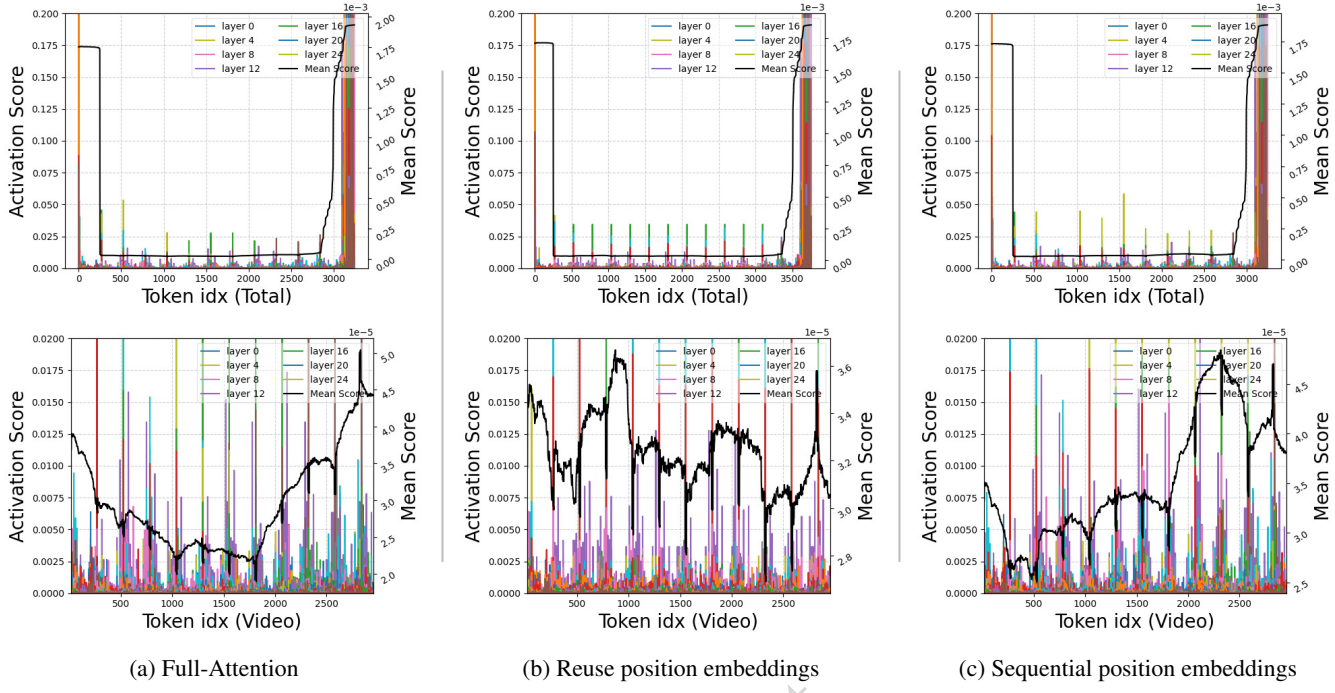


Figure 8: Attention Weight Distributions of LongVILA

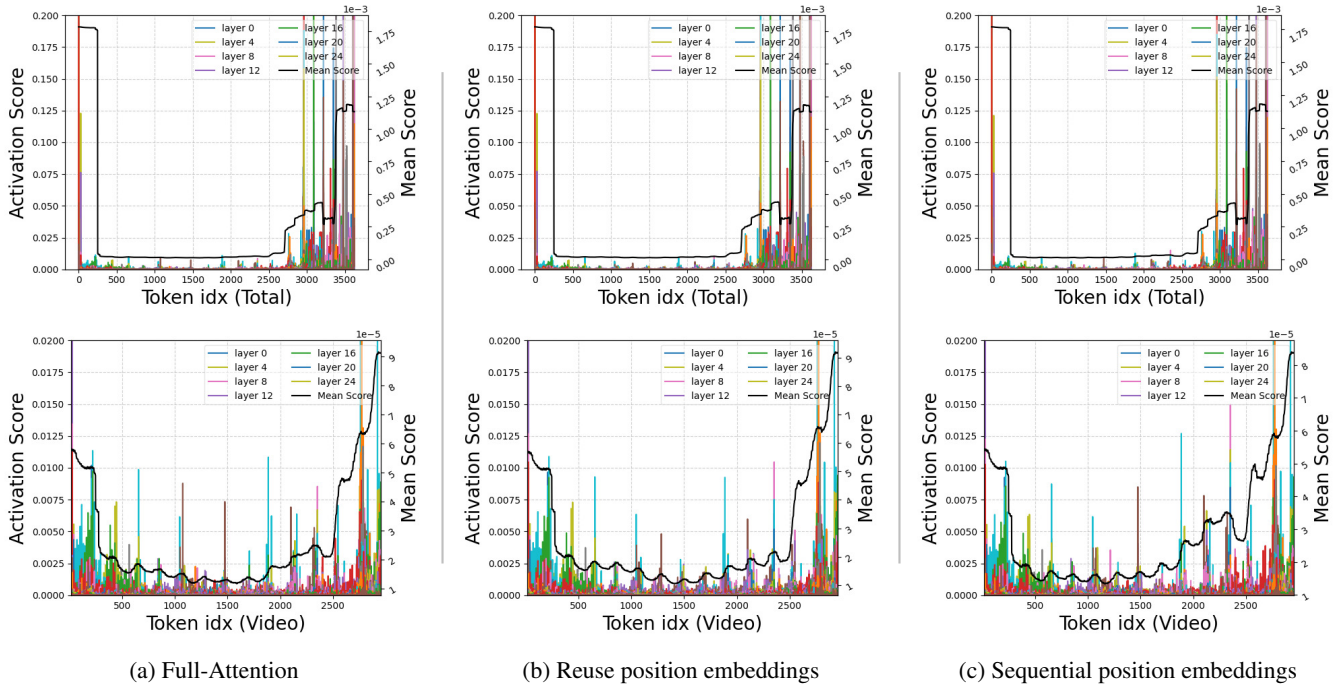


Figure 9: Attention Weight Distributions of LLaVA-Video